ACCOUNTS
of chemical research

Cryogenic Ion Chemistry and Spectroscopy

ARRON B. WOLK,[†] CHRISTOPHER M. LEAVITT,[†]
ETIENNE GARAND,[‡] AND MARK A. JOHNSON*,[†]

[†]*Sterling Chemistry Laboratory, Yale University, P. O. Box 208107, New Haven, Connecticut 06520, United States, and* [‡]*Department of Chemistry, University of Wisconsin, 1101 University Avenue, Madison, Wisconsin 53706, United States*

RECEIVED ON MAY 7, 2013

CONSPECTUS

The use of mass spectrometry in macromolecular analysis is an incredibly important technique and has allowed efficient identification of secondary and tertiary protein structures. Over 20 years ago, Chemistry Nobelist John Fenn and co-workers revolutionized mass spectrometry by developing ways to nondestructively extract large molecules directly from solution into the gas phase. This advance, in turn, enabled rapid sequencing of biopolymers through tandem mass spectrometry at the heart of the burgeoning field of proteomics. In this Account, we discuss how cryogenic cooling, mass selection, and reactive processing together provide a powerful way to characterize ion structures as well as rationally synthesize labile reaction intermediates. This is accomplished by first cooling the ions close to 10 K and condensing onto them weakly bound, chemically inert small molecules or rare gas atoms. This assembly can then be used as a medium in which to quench reactive encounters by rapid evaporation of the adducts, as well as provide a universal means for acquiring highly resolved vibrational action spectra of the embedded species by photoinduced mass loss. Moreover, the spectroscopic measurements can be obtained with readily available, broadly tunable pulsed infrared lasers because absorption of a single photon is sufficient to induce evaporation. We discuss the implementation of these methods with a new type of hybrid photofragmentation mass spectrometer involving two stages of mass selection with two laser excitation regions interfaced to the cryogenic ion source.

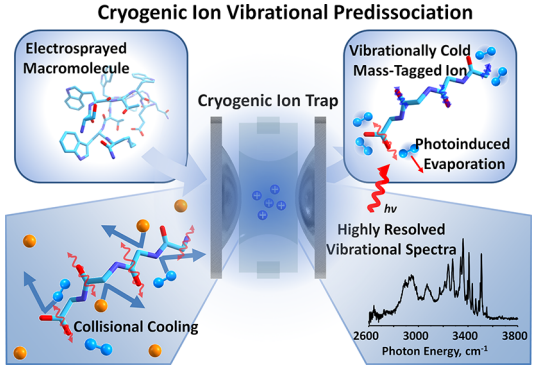

We illustrate several capabilities of the cryogenic ion spectrometer by presenting recent applications to peptides, a biomimetic catalyst, a large antibiotic molecule (vancomycin), and reaction intermediates pertinent to the chemistry of the ionosphere. First, we demonstrate how site-specific isotopic substitution can be used to identify bands due to local functional groups in a protonated tripeptide designed to stereoselectively catalyze bromination of biaryl substrates. This procedure directly reveals the particular H-bond donor and acceptor groups that enforce the folded structure of the bare ion as well as provide contact points for noncovalent interaction with substrates. We then show how photochemical hole-burning involving only vibrational excitations can be used in a double-resonance mode to systematically disentangle overlapping spectra that arise when several conformers of a dipeptide are prepared in the ion source. Finally, we highlight our ability to systematically capture reaction intermediates and spectroscopically characterize their structures. Through this method, we can identify the pathway for water-network-mediated, proton-coupled transformation of nitrosonium, NO^+ to HONO, a key reaction controlling the cations present in the ionosphere. Through this work, we reveal the critical role played by water molecules occupying the second solvation shell around the ion, where they stabilize the emergent product ion in a fashion reminiscent of the solvent coordinate responsible for the barrier to charge transfer in solution. Looking to the future, we predict that the capture and characterization of fleeting intermediate complexes in the homogeneous catalytic activation of small molecules like water, alkanes, and CO_2 is a likely avenue rich with opportunity.

Introduction

The utility of mass spectrometry in macromolecular analysis has undergone a renaissance with the introduction of atmospheric pressure ionization (API) schemes that enable nondestructive access to nonvolatile species and supramolecular assemblies.[1] The practical applications of this capability are perhaps best illustrated by the rise of proteomic analysis,[2] where increasingly sophisticated analysis schemes (MS^n,[3] H/D exchange,[4] ion mobility spectrometry,[5] etc.) have allowed systematic determination of secondary and tertiary

Published on the Web 08/23/2013 www.pubs.acs.org/accounts
10.1021/ar400125a

protein structures.[6] In the meantime, there has been a long-standing effort, largely driven by physical chemists, that has focused on freezing floppy molecules and weakly bound molecular aggregates into well-defined structures and characterizing these entities using electronic or vibrational spectroscopy carried out in an action mode with either IRMPD,[7] UV,[8] UV-IR double resonance[9,10] or "messenger tagging" techniques.[11] This effort was dramatically advanced in the past decade by the interface of API sources to cryogenically cooled multipole ion traps, revealing the intrinsically sharp spectral features of a variety of biologically relevant molecules.[12] In the "messenger tagging" approach, cold ions (A^+) are formed with weakly attached inert species (RG) that are transparent in the infrared (like H_2, N_2, and rare gas atoms). The key is that these $A^+ \cdot RG$ species are readily dissociated upon absorption of a single IR photon resonant with one of the vibrational transitions associated with A^+:

$$A^+ \cdot (RG)_n + h\nu \rightarrow A^+ \cdot (RG)_{n-m} + m RG \qquad (1)$$

so that action spectra *equivalent* to linear absorption spectra can be generally obtained using photodissociation in conjunction with a tandem mass spectrometer.[13] One stage of mass selection is required to isolate the $A^+ \cdot RG_n$ adduct for selective photoexcitation, while a second stage is needed to monitor the lighter A^+ RG_{n-m} photofragment yield as a function of laser excitation frequency. Because action can be recorded upon absorption of a single photon, relatively low-power "table-top" laser systems can easily cover the entire $600-4500\ cm^{-1}$ range of the IR and thus offer a universal means for structural characterization of mass-selected ions. A major alternative to this method is multiphoton dissociation induced by a high-power free electron laser.[7,14]

This cryogenic ion vibrational predissociation (CIVP) strategy was originally carried out using supersonic jet ion sources that readily access temperatures in the 10 K range, yielding structures for many species like hydrated protons,[15] hydrated electrons,[16] and hydroxide ions.[17] More recently, it has been extended to reaction intermediates[18] that are rationally prepared by manipulation of the chemistry uniquely available by carrying out reactions in a cryogenic medium. In the past few years, the scope of chemical processes amenable to study with CIVP has broadened dramatically through the integration of cryogenic (10 K) radio-frequency ion traps with ambient ionization sources,[19] where weakly bound molecules can be readily condensed onto all manner of complex ions. The resulting capability opens the way for a new type of hybrid spectrometer that combines the sensitivity of mass spectrometry with the detailed structural information that can be obtained from optical (vibrational and electronic) spectroscopy. Moreover, chemical and photophysical manipulation of the ions after cooling and adduct formation provides a qualitatively new approach for generation and study of transient intermediates in chemical reactions. This is a holistic approach that integrates the three important capabilities:

1. To freeze flexible assemblies into well-defined structures that yield sharp vibrational spectra
2. To separate contributions from multiple conformers using photochemical hole burning
3. To capture reaction intermediates by evaporative quenching of collision complexes

We present several examples taken from different areas of recent research to illustrate how these principles are being used to provide structural analysis of isolated peptides and drug molecules,[20] as well as to elucidate the detailed role that solvent structure plays in proton-coupled covalent bond formation.[18]

Instrumentation

The essential requirements for CIVP spectroscopy are a source of cold ions and two stages of mass selection so that specific *m/z* target ions can be photoexcited and then the lighter fragment ions can be separated from their intact parents. The scheme developed at Yale over many years, which uses a time-of-flight mass spectrometer as its first analyzer and a modest resolution reflectron as the second, is illustrated in Figure 1. The ion source is on the left, while the laser interaction and mass spectrometry components are on the right.

In the ion source, target species are extracted from solution using electrospray (or other atmospheric ion sources) and transferred using radio-frequency ion guides through three stages of differential pumping to a low pressure region. The warm continuous stream of ions is then injected into a commercial three-dimensional radio-frequency ion trap modified for cryogenic operation and held at 10 K with a closed cycle He cryostat. A seeded buffer gas is pulsed into the trap just prior to ion injection, which contains a trace amount of the cryogenic solvent (e.g., Ar, N_2, H_2, etc.) to be condensed onto the ions after they are collisionally cooled. This growth period takes tens of milliseconds, and relatively large aggregates can be formed depending on the buffer gas pressure and dwell time in the trap. These weakly

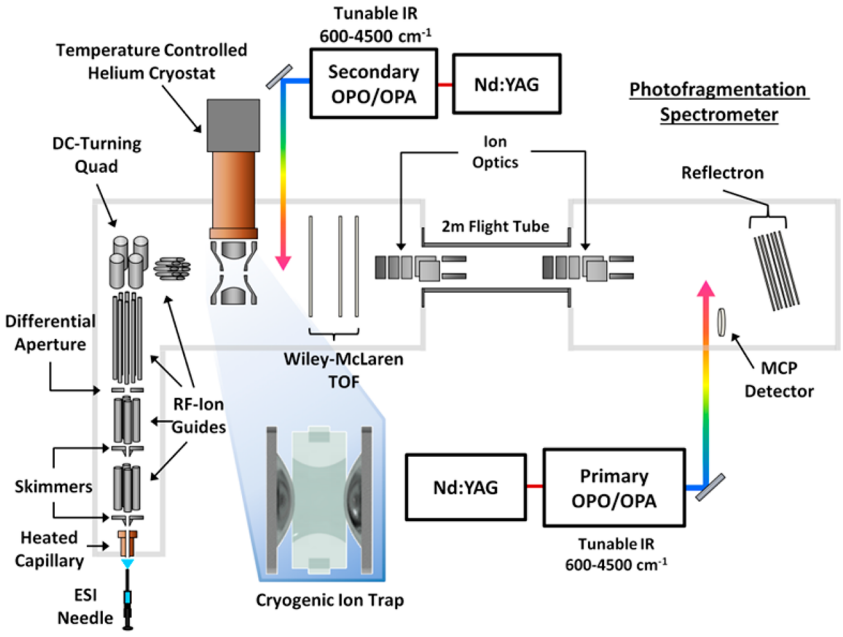

FIGURE 1. In the Yale tandem time-of-flight photofragmentation spectrometer, ions are extracted from solution with electrospray ionization (ESI) and guided into a 10 K 3D quadrapole ion trap. After collisional cooling, ions are extracted from the trap and mass selectively (to unit *m*/*z*) interrogated by one or two pulsed infrared lasers. Primary and secondary lasers are based on optical parametric oscillators and amplifiers (OPO/OPA).

bound solvent molecules typically have little effect on the vibrational spectrum, as evidenced by very small incremental shifts upon addition of the first few molecules.[21] Note that the buffer gas is pulsed into the trap, so that it is slowly evacuated before the ions are extracted. This limits the collisional reheating of the cold ion upon acceleration by the extraction voltages.[22]

Mass spectra illustrating this process are displayed in Figure 2 for the specific case of doubly protonated vancomycin, an antibiotic weighing 1450 Da with the structure included in the inset. With only He in the buffer gas, the mass spectrum simply consists of the bare parent ion that was injected into the trap, stored, and then extracted into the TOF spectrometer described below. When D_2 is added to the buffer, the mass spectra become much more complex as D_2 molecules are attached, accounting for the long series of closely spaced peaks appearing at higher *m*/*z*. The binding energy of D_2 onto an ion is on the order of 500 cm^{-1}, and for a molecule this size, condensation requires cooling the ion from 300 K at the inlet to at least 50 K, which is sufficiently cold to allow the adducts to be kinetically stable on the experimental time scale. Lower buffer gas pressure enhances D_2 aggregation, likely by preserving the larger adducts by limiting collisions upon extraction from the trap. It is likely trivial to grow particles that are so large that they fall out of range of the experimental settings to trap and detect them. Once the ions are coated with a nonreactive,

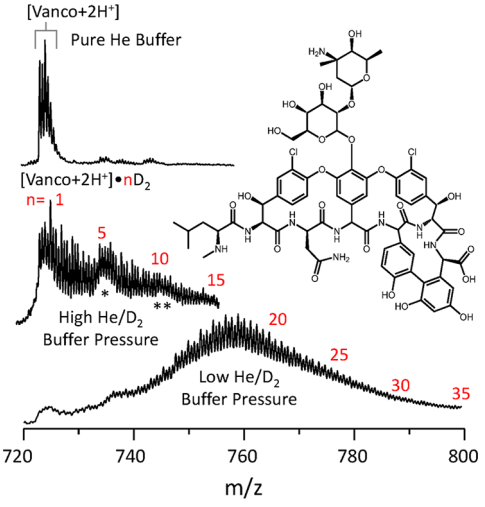

FIGURE 2. Mass spectra illustrating the attachment of dozens of D_2 molecules to the doubly protonated antibiotic molecule, vancomycin, with the structure indicated. The masses indicated with $*$ and $**$ are (Vanco $+ H^+ + Na^+$) and (Vanco $+ 2Na^+$) species, respectively.

cryogenic matrix, this medium creates many new avenues for studying their structure and reactivity, as we illustrate with several examples below.

Tandem time-of-flight methods provide an inexpensive platform for carrying out mass-selective photofragmentation, with a typical arrangement illustrated on the right side of Figure 1. In the basic experiment, a widely tunable IR pulse (10−20 Hz repetition rate, 10 ns pulse width) from the primary laser intercepts a single *m*/*z* ion packet from the ion

distribution arriving from the source. This causes photoevaporation of weakly bound adducts, and the lighter fragment ions are then separated from their parents in a second "reflectron" mass spectrometer and monitored as a function of laser frequency to generate the spectrum. The Yale apparatus also includes a second laser interaction stage (labeled "secondary" in Figure 1), which is used to extract individual spectra when many conformers or isomers appear at the same *m*/*z*. Instruments such as this are not yet commercially available, and several have appeared with subtle variations in a few laboratories around the world.[21,23−25]

Application to Vibrational Spectroscopy

One of the widest and most immediately available applications that exploits cryogenically tagged ions is the acquisition of their vibrational (or electronic) spectra by monitoring photoevaporation of the cryogen. The performance of this approach relies on the fact that the lifetimes of vibrationally excited states are typically on the order of picoseconds before the energy is degraded into heat by anharmonic coupling (often called intramolecular vibrational redistribution, IVR).[26] On the other hand, evaporation of the matrix takes place as a unimolecular decay process and, as such, is governed by RRKM statistical rate theory, which predicts the loss of the matrix molecules to occur on much longer time scales than IVR. An experimental manifestation of this statistical decomposition mechanism is that the number of adduct molecules, *m*, ejected upon absorption of a photon with energy $h\nu$ is typically on the order $h\nu/\Delta H_{evap}$, where ΔH_{evap} is the enthalpy of evaporation of the pure matrix solid.[13,21]

Because of the hierarchy of kinetic processes outlined above, highly resolved vibrational transitions are observed in almost all cases, with typical performance on three systems presented in Figure 3. Traces a and b correspond to the peptides diglycine ($GlyGlyH^+$) and TrpZip (TZ2, a decapeptide), respectively, with their molecular structures displayed in the inset. The lower trace (c) was obtained for doubly protonated vancomycin. Although the bands are obviously much more congested in the larger systems, it appears that the intrinsic line widths of individual features are actually similar in all cases. The most informative functional group transitions for structural analysis are the NH and OH stretching fundamentals highest in energy around 3400 and 3600 cm^{-1} respectively, and the C=O−based bands near 1600 cm^{-1} that are associated with the amide group in peptides as well as ketone and ester motifs in vancomycin. In the simple dipeptide $GlyGlyH^+$, bands

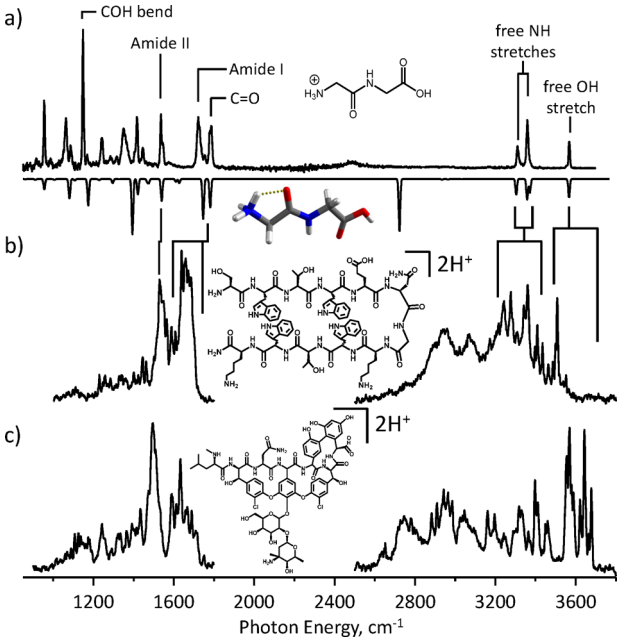

FIGURE 3. The cryogenic ion vibrational predissociation (CIVP) spectrum of (a) the protonated dipeptide $GlyGlyH^+ \cdot (H_2)_2$, (b) the doubly protonated decapeptide $TZ2 \cdot (D_2)_2$, and (c) the doubly protonated antibiotic $vancomycin \cdot (D_2)_2$. The scaled harmonic (MP2/6-311+G(d,p)) spectrum of $GlyGlyH^+$ is inverted below trace a) for comparison. The principal energy ranges for common vibrational chromophores are indicated at the top.

associated with each of these groups are cleanly resolved as indicated at the top of Figure 3a.

For the small $GlyGlyH^+$ system, the vast majority of the CIVP features can be accurately predicted by the harmonic spectrum calculated for the minimum energy structure presented as the inverted trace below the experimental spectrum. This structure features a cyclic intramolecular H-bond involving a coupling between the NH_3^+ N-terminus and the nearby amide C=O, which acts to red-shift both donor and acceptor constituents of this H-bond linkage. Other strong bands are clearly evident that are not expected at the harmonic level but that are especially important because they encode the anharmonic interactions arising from the complex potential energy landscape of the peptide hypersurface. Such spectral information is only now becoming available through this type of measurement, providing stringent experimental benchmarks for simulations aimed to explain and predict the behavior of much larger systems at finite temperature.[27]

Band Assignments of Congested Spectra through Site-Specific Isotopic Substitution

The behavior of the simple dipeptide $GlyGlyH^+$ displayed in Figure 3a establishes that transitions associated with particular functional groups appear as sharp features that are

readily assigned when they are, as in this case, well dispersed throughout the spectrum. The more typical situation, however, is that found in the larger TrpZip and vancomycin ions (Figure 3b,c), in which many similar groups give rise to strongly overlapping or even (at least for TrpZip[28,29]) intrinsically coupled bands. For example, in vancomycin (Figure 3c), a cursory inspection of the congested C=O, NH, and OH stretching regions reveals distinct substructure that is consistent with independent contributions from a majority of these groups in the molecules, while the individual contributions in TrpZip are less clear (Figure 3b). In such cases, obtaining the detailed assignments required for structure determination requires a method that can identify whether particular functional groups can indeed be traced to specific, sharp transitions embedded in congested regions of the spectrum (as opposed to collective motions involving delocalized motion spread throughout the molecule). It would be particularly useful, for example, if one could isolate the vibrational frequencies of embedded oscillators due to key chemical bonds and use them as reporters on their local chemical environments. This type of information is typically obtained in NMR through site-specific isotopic substitution, and analogous isotopic schemes are used to deconvolute the broad IR and Raman bands displayed by peptides and proteins.[30] When applied to ions in the cryogenic environment, one can exploit the fact that the transitions are intrinsically narrow to obtain such site-specific information with unprecedented accuracy. This approach was pioneered in the gas phase by Rizzo and co-workers in the analysis of cryogenic polyalanine helices.[31]

The basic idea of "isotope-edited" vibrational spectroscopy is to empirically identify the carriers of spectral activity in a particular region of the spectrum by taking differences between the spectrum obtained when the target molecule has all isotopes present in their dominant form and that obtained when the same molecule is prepared with one atomic site replaced by its heavier isotope. Figure 4 presents several such "isotope edited" difference spectra for a synthetic tripeptide substituted at several key sites as indicated in the structure at the top right. This molecule is a catalyst designed to achieve biomimetic stereoselective bromination of small biaryl substrates.[32] The C=O bands between 1600 and 1750 cm^{-1} are particularly informative, because four of these appear in the spectrum of the dominant (normal) isotopomer displayed in the bottom trace, suggesting that each C=O in the peptide might contribute one of these transitions to the spectrum in a scenario where the cold molecule adopts a single, well-defined conformation. The four C=O transitions occur as two separated doublets, with the lower energy pair falling about 90 cm^{-1} below the upper pair. We note that red-shifted C=O bands typically occur when this group is involved in an acceptor role for intramolecular H-bonding.

The isotope-edited difference spectra for incorporation of ^{13}C in two of the C=O groups (the so-called BOC group (green) and the terminal tertiary amide (red)) immediately reveal the bands associated with each position through the telltale pseudoderivative line shapes. Positive going peaks indicate transitions lost upon incorporation of the heavy isotope, while the negative companion peak indicates new features that appear with it. The most striking feature of this peptide's behavior is that only one transition is significantly affected within each signature region (amide I, amide II, and NH stretch), thus allowing immediate identification of the *local* oscillators mostly responsible for each transition. Note that more than one spectral region may be affected by a single substitution, which is most obvious in the case of the ^{15}N substitution at the embedded amide (orange), where both the NH stretch at 3345 cm^{-1} and the CN amide II band at 1516 cm^{-1} are strongly affected. Interestingly, the magnitudes of the shifts between the positive and negative peaks provides a direct measurement of the degree to which the labeled atoms contribute to the collective normal modes associated with specific transitions. In this case, the C=O bands (green and red) exhibit almost limiting shifts that would be expected for participation of only the diatomic displacement, which is governed by the square root of the reduced mass of the two atom system (36 cm^{-1} near the center of the amide I region). Since the observed shifts for the BOC (green) and amide (red) are 36 and 35 cm^{-1}, respectively, very close to the limiting value, we conclude that the local bond displacements are indeed largely responsible for the observed bands. Thus, the C=O and NH transition energies indeed reflect the chemical environments of particular functional groups, which are then color-coded with the upper schematic structure in Figure 4.

The locations of the fundamentals associated with the key NH and C=O bonds obtained through the difference spectra provide a direct diagnostic for the groups involved in intramolecular H-bonding. As discussed above, we expect red shifts of the frequencies of both NH donor and C=O acceptor groups over the range indicated by the color bars in the lower trace of Figure 4. The two red-shifted carbonyl groups (red and blue) are thus identified as H-bond acceptors, while one of the two NH groups (orange) acts a donor. The free NH is then assigned to the remaining position on

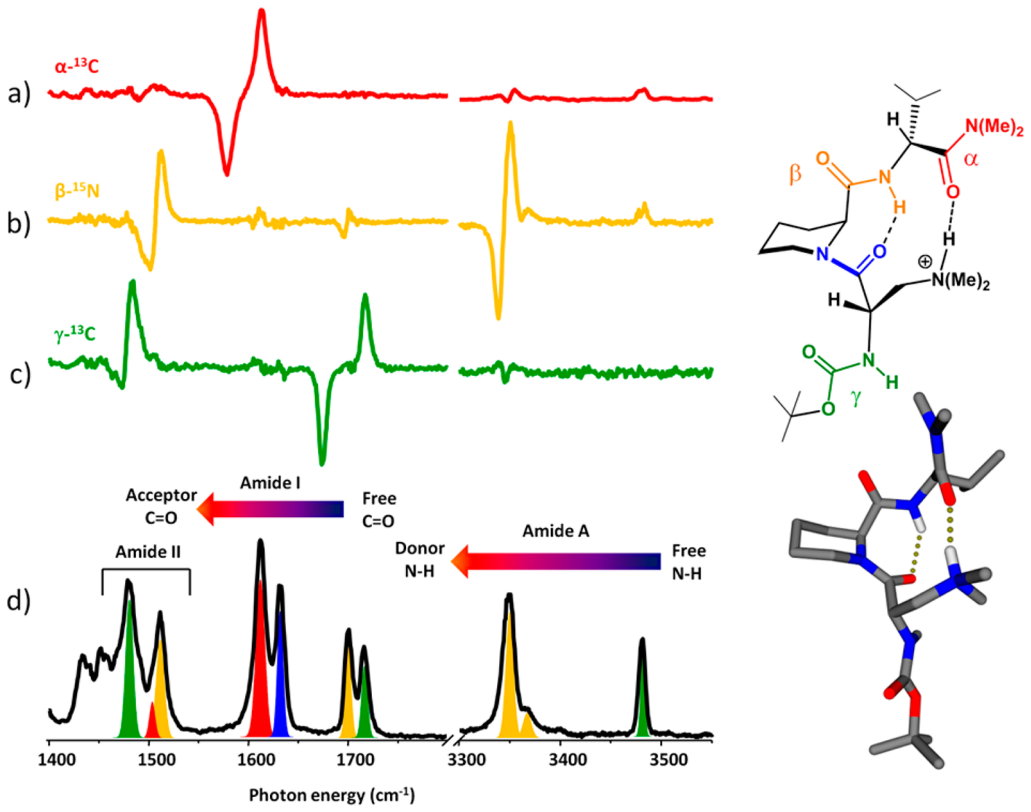

FIGURE 4. Band assignments in a tripeptide spectrum through site-specific isotopic substitution. The groups contributing to various CIVP bands in panel d) are color-coded with skeletal structure on top right. Upper traces a), b), and c) are difference spectra depicting changes caused by placing heavy isotopes in the sites labeled α, β, and γ in the upper right structure.

the BOC group (green). This information provides a sufficiently stringent set of constraints to easily identify the conformational type at play by comparison with harmonic spectra calculated for various minima on the complex potential energy surface. The particular folded, double H-bonded topology of this tripeptide is displayed in the lower trace in Figure 4.

Although it is indeed labor intensive to create a library of catalyst molecules with labels in all the critical sites, once available, this set can be used to systematically identify the specific contact points through which the multidentate catalyst host noncovalently captures guest molecules. This was demonstrated[32] for capture of both an alkali ion (Na^+) and a biaryl guest, where the latter application required isotopic labels on both the catalyst and the substrate.

Isomer-Selective Spectra When Multiple Conformers Occur at a Particular Mass

The examples presented above illustrate how structural information can be obtained from CIVP spectra of the cold ions when only one form is created in the cryogenic trap. It is much more common, however, and especially so in its application to floppy biopolymers like polypeptides, that many isomers (protonation site variation, for example) or conformers (rotation around amide bonds, etc.) are either extracted from solution or prepared under the trapping conditions[5] such that the vibrational spectrum of a particular mass would consist of many overlapping spectra. In cases where one of the constituents possesses an electronic chromophore, there are many strategies to carry out conformer-selective spectroscopy based on IR-UV double resonance.[9,10,33] One can also achieve conformer selectivity by exploiting differences in the vibrational band patterns of the conformers using an IR–IR double resonance approach as we illustrate below.[34]

Conformer-selective CIVP spectroscopy relies on the fact the resonant IR absorption by a tagged ion leads to the loss of this *m/z* parent ion through the same photofragmentation process used to detect its vibrational spectrum. This destructive event provides a natural photochemical "hole burning" scheme with which to selectively remove one of the conformers from an ensemble, provided there is at least one transition that is accidentally isolated from those arising from the other species.

Figure 5 presents an example where individual spectra are systematically extracted from a mixture of conformers

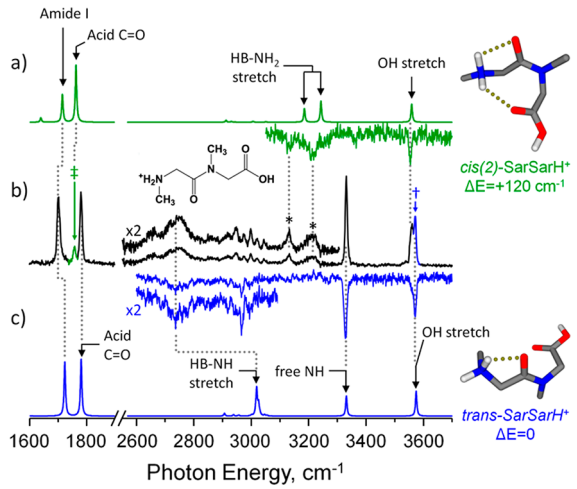

FIGURE 5. Extraction of the individual spectra of two conformers in the dipeptide SarSarH$^+$ with IR–IR double resonance. The CIVP spectrum in part b is resolved into the two contributions (dip spectra in parts a and c) by setting the probe laser on the colored transitions indicated († and ‡) and scanning the pump laser. The two conformers are shown on the right along with their harmonic spectra (MP2/6-311+G(d,p)).

involving the SarSarH$^+$ dipeptide, a dimethylated variation of the GlyGlyH$^+$ system discussed above. At high energy, we again find bands arising from the free NH and OH groups as indicated, but the OH feature is clearly split into a doublet, while a very broad set of transitions lie just below the free NH band at 3132 and 3195 cm^{-1}, respectively (∗ in Figure 5b). In addition, the C=O region includes a sharp interloper (‡) just below the carbonyl associated with the acid group. As discussed above in our analysis of the catalyst spectrum, such red shifting often reflects internal H-bonding, pointing to a conformer where the C=O group on the acid plays an acceptor role. If that assignment is correct, then both terminal NH groups must be involved in H-bonds, since one NH is already attached to the amide in the ring motif identified in the GlyGlyH$^+$ ion, and the OH doublet (†) lies too high in energy to be involved as the H-bond donor.

This hypothetical assignment of the weaker C=O feature (‡) to an intramolecular H-bond can be proven using IR–IR double resonance by fixing the pump laser on the ‡ transition and continuously monitoring the fragment signal while the pump laser is scanned through the higher energy range of the NH stretches. The probe signal monitors the population of the conformer responsible for the ‡ band, and the key to the hole-burning method is to intersect the same ion packet with a powerful pump laser before it interacts with the probe. When the pump laser drives *any* of the transitions associated with the conformer being isolated with the probe transition, its population will be removed by photoevaporation of its adducts. Thus, the *entire* spectrum associated with the conformer selected by the probe is revealed by "dips" in the probe fragment signal as the pump laser is scanned through the spectrum.

The green trace in Figure 5 presents the hole-burning spectrum obtained when the probe laser was fixed on the weak C=O band (‡). Note that the strong free NH band at 3333 cm^{-1} is indeed missing in this dip spectrum, while the two weaker features (∗) at 3132 and 3195 cm^{-1} are present, in addition to a single free OH feature traced to the acid group. This pattern indicates that it arises from a conformer in which both NH groups on the N-terminus are engaged as H-bond donors, and the structure displayed in the inset was found to be a local minimum with the predicted harmonic spectrum presented just above the dip trace. The two red-shifted bands (∗) are thus traced to the coupled modes of an embedded $-NH_2$ group with both hydrogen atoms attached to nearby C=O groups, which in turn lead to red shifts of both C=O transitions.

Extending this strategy revealed another conformer with a single internal H-bond, consistent with the *trans*-SarSarH$^+$ structure displayed in Figure 5c. Thus, through systematic choice of probe transitions, we can disentangle overlapping bands to reveal the independent spectra of each conformer generated by the ion source. We note that this capability is general and has been used, for example, in conjunction with isotope labeling described above to extract the contributions of individual water molecules embedded in various sites of an extended network.[35]

Putting It All Together: Isolation and Vibrational Characterization of Reaction Intermediates

Thus far, we have focused on the spectroscopic capabilities created by combining photofragmentation mass spectrometry with cryogenic processing of the target ion. Once a reactant ion is embedded in the cryogenic medium, however, one can also use this assembly to condense a reactant molecule and quench the activated collision complex into shallow minima, thus trapping intermediates along a reaction pathway. Although this aspect of cryogenic ion chemistry is still in its infancy, an excellent example of the evaporative capture of reaction intermediates is afforded by the recent study[18] of the water cluster-mediated transformation of nitrosonium to nitrous acid,

$$NO^+ + 4H_2O \rightarrow HONO + H^+ \cdot (H_2O)_3 \qquad (2)$$

a key reaction controlling the ambient cation distribution present in Earth's ionosphere. The mechanism is known

to require three water molecules to proceed such that two water molecules play a catalytic role. There was a long-standing puzzle, however, regarding how the tiny network of molecules had to be arranged to facilitate covalent N−O bond formation with concomitant charge translocation onto the ionic product, a protonated water cluster. The critical intermediate network structures along the reaction path were trapped using cryogenic ion chemistry in which the NO^+ reactant ion was first embedded in a large Ar cluster and then water molecules were sequentially added by Ar-mediated condensation:

$$NO^+\cdot(H_2O)_n\cdot Ar_p + H_2O \rightarrow (NO^+\cdot(H_2O)_{(n+1)})^* \cdot Ar_p \rightarrow (NO^+\cdot(H_2O)_{(n+1)})\cdot Ar_q + (p-q)\cdot Ar \quad (3)$$

The reaction intermediates then occur as isomers with composition $(NO^+\cdot(H_2O)_{n+1})$. Once again, the hierarchy of relaxation events following condensation is crucial for successful sampling of the reactive potential energy before the activated complexes are quenched into local minima. For hydrogen-bonded networks, this time scale is on the order of picoseconds,[36] while the evaporation of the weakly bound Ar atoms occurs on the much longer time scales of tens to hundreds of picoseconds.

The hole-burning scheme described above was used to identify the spectral patterns of three intermediates recovered in the CIVP spectrum of the trihydrate, displayed in Figure 6. The three contributions are color-coded and were analyzed to identify the water network structures by comparison with their predicted vibrational patterns. The most unreactive form features all three water molecules in the first hydration shell with the structure labeled α, where each water molecule directly contacts the NO^+ ion. The reaction begins to occur when one water molecule moves to the second solvation shell to form the diamond structure β, while the most reactive form features two water molecules in the second solvation shell with structure γ. The γ (blue) isomer exhibits the most red-shifted NO^+ and OH stretches, which track the delocalization of the charge from the NO^+ moiety onto the water network. Thus, the evolution along the reaction coordinate is associated with sequential migration of water molecules from the first to the second solvation shell. Although the forms β and γ, with water molecules more remote from the ion, are calculated to be higher in energy, they promote reaction by providing the correct hydration environment to accommodate the charge build up on water in the product state. Note that these higher

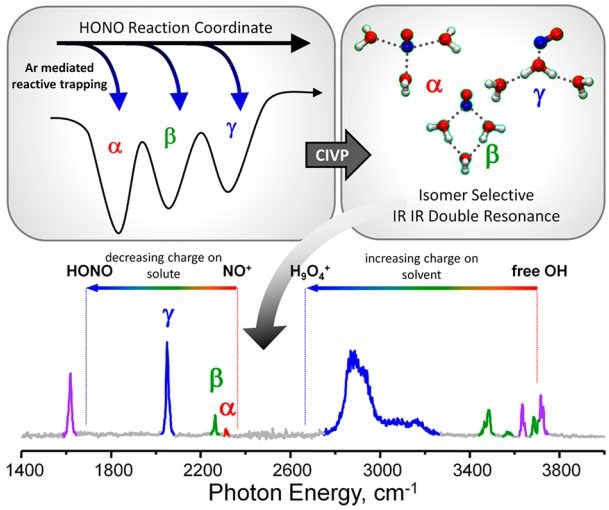

FIGURE 6. Trapping reactive intermediates in the water-catalyzed $NO^+ + H_2O \rightarrow HONO + H^+$ reaction. Rapid evaporation of Ar atoms when H_2O is condensed onto the $NO^+(H_2O)_2\cdot Ar_{n>5}$ reactant quenches $NO^+(H_2O)_3$ into three distinct species in the pathway toward products. IR−IR double-resonance reveals the spectra of the three intermediates (α, β, and γ), as color-coded in the CIVP spectrum (the purple OH transitions are shared by both α and γ, and the band at 1600 cm^{-1} is shared by all three isomers). Color bars indicate location of bands relative to the signatures of asymptotic reactants and products. The structures of the three species (upper right) indicate that the reaction proceeds by sequential displacement of a water molecule from the first to the second hydration shell around the reactant ion.

energy forms are efficiently trapped using cryogenic condensation, a necessary requirement for the utility of this method to study more complex reaction intermediates.

In summary, we see a rapidly expanding range of possibilities where the combination of cold ion chemistry and spectroscopy can be used to shed new light on processes and species that have proven to be too fleeting to be characterized with traditional means of chemical analysis. It is indeed anticipated that such processing techniques can also freeze larger biological assemblies, representing a logical direction for extension of the method. The capture of very highly reactive transients in the final steps of small molecule activation, such as water oxidation and CO_2 reduction, appears to be a particularly attractive area where such measurements will have immediate and high impact on catalyst design.

This research is funded by the Air Force Office of Scientific Research under Grant FA9550-09-1-0139 and the National Science Foundation under Grant CHE-1213634.

BIOGRAPHICAL INFORMATION

Arron B. Wolk received his B.A. in Chemistry from Colorado College in 2009 and is currently a graduate student at Yale

University. His research focuses on developing and applying cryogenic ion processing for the characterization of hydrogen bonding motifs in macromolecules and activated organometallic catalysts.

Christopher M. Leavitt received his B.S. degree in Chemistry at Wichita State University in 2008 and his Ph.D. from Yale University in 2013 with Mark A. Johnson where his research focused on the identification of hydrogen bonding motifs in ionic systems. He is currently a postdoctoral researcher at the University of Georgia in the laboratory of Gary E. Douberly.

Etienne Garand is currently an assistant professor at the University of Wisconsin—Madison. He received his Ph.D. from the University of California, Berkeley (2010), and did his postdoctoral work at Yale University (2012). His current research interests are focused on the isolation and characterization of catalytic reaction intermediates.

Mark A. Johnson is the Arthur T. Kemp Professor of Chemistry at Yale University. His research interests focus on the isolation of reactive intermediates and characterization of hydrogen bonding motifs in cluster and electrosprayed ions. Recently, he was elected into the American Academy of Arts and Sciences (2009) and received the Humboldt Senior Research Award (2012).

FOOTNOTES

The authors declare no competing financial interest.

REFERENCES

1 Ifa, D. R.; Wu, C. P.; Ouyang, Z.; Cooks, R. G. Desorption Electrospray Ionization and Other Ambient Ionization Methods: Current Progress and Preview. *Analyst* **2010**, *135*, 669–681.

2 Reid, G. E.; McLuckey, S. A. 'Top Down' Protein Characterization via Tandem Mass Spectrometry. *J. Mass Spectrom.* **2002**, *37*, 663–675.

3 Tsaprailis, G.; Nair, H.; Somogyi, A.; Wysocki, V. H.; Zhong, W. Q.; Futrell, J. H.; Summerfield, S. G.; Gaskell, S. J. Influence of Secondary Structure on the Fragmentation of Protonated Peptides. *J. Am. Chem. Soc.* **1999**, *121*, 5142–5154.

4 Campbell, S.; Rodgers, M. T.; Marzluff, E. M.; Beauchamp, J. L. Deuterium Exchange Reactions as a Probe of Biomolecule Structure. Fundamental studies of gas phase H/D exchange reactions of protonated glycine oligomers with D_2O, CD_3OD, and CD_3CO_2D, and ND_3. *J. Am. Chem. Soc.* **1995**, *117*, 12840–12854.

5 Bohrer, B. C.; Mererbloom, S. I.; Koeniger, S. L.; Hilderbrand, A. E.; Clemmer, D. E. Biomolecule Analysis by Ion Mobility Spectrometry. *Annu. Rev. Anal. Chem.* **2008**, *1*, 293–327.

6 Hall, Z.; Politis, A.; Robinson, C. V. Structural Modeling of Heteromeric Protein Complexes from Disassembly Pathways and Ion Mobility-Mass Spectrometry. *Structure* **2012**, *20*, 1596–1609.

7 Polfer, N. C.; Oomens, J. Vibrational Spectroscopy of Bare and Solvated Ionic Complexes of Biological Relevance. *Mass Spectrom. Rev.* **2009**, *28*, 468–494.

8 Chakrabarty, S.; Rudnev, V.; Fulara, J.; Dietsche, R.; Nagy, A.; Garkusha, I.; Mazzotti, F. J.; Rice, C. A.; Maier, J. P. Electronic spectra of $C_4H_3Cl^+$ isomers. *Mol. Phys.* **2012**, *110*, 3077–3084.

9 Dean, J. C.; Buchanan, E. G.; Zwier, T. S. Mixed 14/16 Helices in the Gas Phase: Conformation-Specific Spectroscopy of Z-$(Gly)_n$, n = 1, 3, 5. *J. Am. Chem. Soc.* **2012**, *134*, 17186–17201.

10 Nagornova, N. S.; Rizzo, T. R.; Boyarkin, O. V. Interplay of Intra- and Intermolecular H-bonding in a Progressively Solvated Macrocyclic Peptide. *Science* **2012**, *336*, 320–323.

11 Okumura, M.; Yeh, L. I.; Myers, J. D.; Lee, Y. T. Infrared Spectra of the Cluster Ions $H_7O_3^+ \cdot H_2$ and $H_9O_4^+ \cdot H_2$. *J. Chem. Phys.* **1986**, *85*, 2328–2329.

12 Boyarkin, O. V.; Mercier, S. R.; Kamariotis, A.; Rizzo, T. R. Electronic Spectroscopy of Cold, Protonated Tryptophan and Tyrosine. *J. Am. Chem. Soc.* **2006**, *128*, 2816–2817.

13 Johnson, M. A. Vibrational Predissociation Ion Spectroscopy. In *Encyclopedia of Mass Spectrometry*; Armentrout, P. B., Gross, M. L., Caprioli, R., Eds.; Elsevier: Amsterdam, 2003, Vol. 1.

14 Lemaire, J.; Boissel, P.; Heninger, M.; Mauclaire, G.; Bellec, G.; Mestdagh, H.; Simon, A.; Caer, S. L.; Ortega, J. M.; Glotin, F.; Maitre, P. Gas Phase Infrared Spectroscopy of Selectively Prepared Ions. *Phys. Rev. Lett.* **2002**, *89*, No. 273002.

15 Headrick, J. M.; Diken, E. G.; Walters, R. S.; Hammer, N. I.; Christie, R. A.; Cui, J.; Myshakin, E. M.; Duncan, M. A.; Johnson, M. A.; Jordan, K. D. Spectral Signatures of Hydrated Proton Vibrations in Water Clusters. *Science* **2005**, *308*, 1765–1769.

16 Hammer, N. I.; Shin, J.-W.; Headrick, J. M.; Diken, E. G.; Roscioli, J. R.; Weddle, G. H.; Johnson, M. A. How Do Small Water Clusters Bind an Excess Electron? *Science* **2004**, *306*, 675–679.

17 Robertson, W. H.; Diken, E. G.; Price, E. A.; Shin, J.-W.; Johnson, M. A. Spectroscopic Determination of the OH Solvation Shell in the $OH^-(H_2O)_n$ Clusters. *Science* **2003**, *299*, 1367.

18 Relph, R. A.; Guasco, T. L.; Elliott, B. M.; Kamrath, M. Z.; McCoy, A. B.; Steele, R. P.; Schofield, D. P.; Jordan, K. D.; Viggiano, A. A.; Ferguson, E. E.; Johnson, M. A. How the Shape of an H-Bonded Network Controls Proton-Coupled Water Activation in HONO Formation. *Science* **2010**, *327*, 308–312.

19 Wang, X. B.; Xing, X. P.; Wang, L. S. Observation of H_2 Aggregation onto a Doubly Charged Anion in a Temperature-Controlled Ion Trap. *J. Phys. Chem. A* **2008**, *112*, 13271–13274.

20 Leavitt, C. M.; Wolk, A. B.; Kamrath, M. Z.; Garand, E.; van Stipdonk, M. J.; Johnson, M. A. Characterizing the Intramolecular H-bond and Secondary Structure in Methylated $GlyGlyH^+$ with H_2 Predissociation Spectroscopy. *J. Am. Soc. Mass Spectrom.* **2011**, *22*, 1941–1952.

21 Kamrath, M. Z.; Garand, E.; Jordan, P. A.; Leavitt, C. M.; Wolk, A. B.; Van Stipdonk, M. J.; Miller, S. J.; Johnson, M. A. Vibrational Characterization of Simple Peptides Using Cryogenic Infrared Photodissociation of H_2-Tagged, Mass-Selected Ions. *J. Am. Chem. Soc.* **2011**, *133*, 6440–6448.

22 Drahos, L.; Vekey, K. MassKinetics: A Theoretical Model of Mass Spectra Incorporating Physical Processes, Reaction Kinetics and Mathematical Descriptions. *J. Mass Spectrom.* **2001**, *36*, 237–263.

23 Goebbert, D. J.; Meijer, G.; Asmis, K. R. 10K Ring Electrode Trap - Tandem Mass Spectrometer for Infrared Spectroscopy of Mass Selected Ions. *AIP Conf. Proc.* **2009**, *1104*, 22–29.

24 Kim, J. B.; Hock, C.; Yacovitch, T. I.; Neumark, D. M. Slow Photoelectron Velocity-Map Imaging of Cold Thiozonide (S_3^-). *J. Phys. Chem. A* **201310.1021/jp401083u.**

25 Wang, Y.-S.; Tsai, C.-H.; Lee, Y. T.; Chang, H.-C.; Jiang, J. C.; Asvany, O.; Schlemmer, S.; Gerlich, D. Investigations of Protonated and Deprotonated Water Clusters Using a Low-Temperature 22-Pole Ion Trap. *J. Phys. Chem. A* **2003**, *107*, 4217–4225.

26 Nesbitt, D. J.; Field, R. W. Vibrational Energy Flow in Highly Excited Molecules: Role of intramolecular vibrational redistribution. *J. Phys. Chem.* **1996**, *100*, 12735–12756.

27 Wang, L.; Middleton, C. T.; Zanni, M. T.; Skinner, J. L. Development and Validation of Transferable Amide I Vibrational Frequency Maps for Peptides. *J. Phys. Chem. B* **2011**, *115*, 3713–3724.

28 Wang, J. P.; Chen, J. X.; Hochstrasser, R. M. Local Structure of β-Hairpin Isotopomers by FTIR, 2D IR, and Ab Initio Theory. *J. Phys. Chem. B* **2006**, *110*, 7545–7555.

29 Smith, A. W.; Lessing, J.; Ganim, Z.; Peng, C. S.; Tokmakoff, A.; Roy, S.; Jansen, T. L. C.; Knoester, J. Melting of a β-Hairpin Peptide Using Isotope-Edited 2D IR Spectroscopy and Simulations. *J. Phys. Chem. B* **2010**, *114*, 10913–10924.

30 Decatur, S. M. Elucidation of Residue-Level Structure and Dynamics of Polypeptides via Isotope-Edited Infrared Spectroscopy. *Acc. Chem. Res.* **2006**, *39*, 169–175.

31 Rizzo, T. R.; Stearns, J. A.; Boyarkin, O. V. Spectroscopic Studies of Cold, Gas-Phase Biomolecular Ions. *Int. Rev. Phys. Chem.* **2009**, *28*, 481–515.

32 Garand, E.; Kamrath, M. Z.; Jordan, P. A.; Wolk, A. B.; Leavitt, C. M.; McCoy, A. B.; Miller, S. J.; Johnson, M. A. Determination of Noncovalent Docking by Infrared Spectroscopy of Cold Gas-phase Complexes. *Science* **2012**, *335*, 694–698.

33 Brenner, V.; Piuzzi, F.; Dimicoli, I.; Tardivel, B.; Mons, M. Chirality-Controlled Formation of beta-Turn Secondary Structures in Short Peptide Chains: Gas-Phase Experiment versus Quantum Chemistry. *Angew. Chem., Int. Ed.* **2007**, *46*, 2463–2466.

34 Leavitt, C. M.; Wolk, A. B.; Fournier, J. A.; Kamrath, M. Z.; Garand, E.; Van Stipdonk, M. J.; Johnson, M. A. Isomer-Specific IR—IR Double Resonance Spectroscopy of D_2-tagged Protonated Dipeptides Prepared in a Cryogenic Ion Trap. *J. Phys. Chem. Lett.* **2012**, *3*, 1099–1105.

35 Guasco, T. L.; Elliott, B. M.; Johnson, M. A.; Ding, J.; Jordan, K. D. Isolating the Spectral Signatures of Individual Sites in Water Networks using Vibrational Double-resonance Spectroscopy of Cluster Isotopomers. *J. Phys. Chem. Lett.* **2010**, *1*, 2396–2401.

36 Tanabe, K.; Miyazaki, M.; Schmies, M.; Patzer, A.; Schutz, M.; Sekiya, H.; Sakai, M.; Dopfer, O.; Fujii, M. Watching Water Migration around a Peptide Bond. *Angew. Chem., Int. Ed.* **2012**, *51*, 6604–6607.